Microstructure and interface analysis of emerging Ga(Sb,Bi) epilayers and Ga(Sb,Bi)/GaSb quantum wells for optoelectronic applications

E. Luna, O. Delorme, L. Cerutti, E. Tournié, J.-B. Rodriguez, A. Trampert

Microstructure and interface analysis of emerging Ga(Sb,Bi) epilayers and Ga(Sb,Bi)/GaSb quantum wells for optoelectronic applications

E. Luna,[1,a)] O. Delorme,[2] L. Cerutti,[2] E. Tournié,[2] J.-B. Rodriguez,[2] and A. Trampert[1]
[1]*Paul-Drude-Institut für Festkörperelektronik, Leibniz-Institut im Forschungsverbund Berlin e.V., Hausvogteiplatz 5-7, D-10117 Berlin, Germany*
[2]*IES, Université de Montpellier, CNRS, F-34000 Montpellier, France*

(Received 30 January 2018; accepted 21 March 2018; published online 10 April 2018)

Using transmission electron microscopy, we present an in-depth microstructural analysis of a series of Ga(Sb,Bi) epilayers and Ga(Sb,Bi)/GaSb quantum wells grown on GaSb(001) substrates by molecular beam epitaxy. Despite the dilute bismide compound Ga(Sb,Bi) is regarded as a highly-mismatched alloy, we find that the material is of remarkable structural perfection, even up to 11%–14% Bi, the maximum Bi concentration incorporated into GaSb so far. No extended defects, nanoclusters, or composition modulations are detectable in the pseudomorphic layers. In addition, the quantum wells exhibit regular and homogeneous morphologies including smooth and stable interfaces with a chemical width on the same order as in other high-quality III–V heterointerfaces. These results may give reasons for the recent successful realization of mid-infrared lasers with room temperature operation based on the very same quantum well structures. *Published by AIP Publishing.* https://doi.org/10.1063/1.5024199

The development of III-V-Bi compounds has recently emerged as a strong research field in semiconductor science and technology.[1] This is mainly due to the unique properties of dilute bismides, such as the large bandgap reduction and spin-orbit splitting energy increase upon the incorporation of a few percent Bi.[2] Due to the narrow bandgap of GaSb (0.725 eV at room temperature), Ga(Sb,Bi) alloys are good candidates for optoelectronic devices operating in the 2–5 μm mid-infrared (mid-IR) range, as recently confirmed by the demonstration of the first laser based on Ga(Sb,Bi)/GaSb quantum wells (QWs) with mid-IR emission at low and room temperatures.[3]

III-V-Bi compounds are highly-mismatched alloys (HMAs), which are formed by the isoelectronic substitution of elements with very different sizes and/or electronegativity in the anion sublattice. As a consequence, HMAs are often affected by miscibility gaps, which makes their growth challenging due to the phase separation tendency of the alloy. Extensive work on other HMA systems (e.g., dilute group-III nitrides) evidenced that composition fluctuations and morphological instabilities have a detrimental effect on the optical response and limit further optoelectronic applications.[4] Among Bi-containing III–V semiconductors, Ga(As,Bi) is the most investigated material, and recent works report morphological instabilities, clustering, and composition modulations (CMs) depending on the specific growth conditions.[5–9] On the contrary, GaSb compounds alloyed with Bi have been far less studied (the first reports on the alloy date back to 2012),[10,11] and questions such as alloy stability, segregation, or solubility limits are still unexplored. In spite of the recent demonstration of laser emission, material developments are still required for the further use of Ga(Sb,Bi) in practical devices. As an example of the current limit, the photoluminescence emission from Ga(Sb,Bi)/GaSb QWs is still broad. On the other hand, although the mismatch in the atomic radius and electronegativity between Sb and Bi is smaller than that between As and Bi and thus a higher solubility of Bi into GaSb than that of Bi into GaAs is expected, the incorporation mechanisms and solubility limits of Bi into GaSb are unknown. Furthermore, to what extent Ga(Sb,Bi) can be even referred to as HMA is still unclear. To date, and after overcoming the initial difficulties in incorporating Bi into GaSb of the earliest works,[10,11] the maximum Bi incorporated in GaSb is about 14%,[12] which is smaller than the reported maximum 21% Bi incorporation into GaAs.[13] Hence, addressing these fundamental questions will allow the further development of Ga(Sb,Bi)-based devices.

At present, most of the few published works on Ga(Sb,Bi) focus on the growth by molecular beam epitaxy (MBE) of the material to explore the growth parameters controlling Bi incorporation.[11,14–17] The assessment of the quality of the samples is commonly based on X-ray diffraction (XRD), atomic force microscopy, scanning electron microscopy, and optical spectroscopy measurements.[11,14–19] The Bi composition is mainly determined using Rutherford backscattering spectroscopy (RBS).[11,14–18] Surprisingly, there is an obvious lack of information on the samples' microstructure determined using transmission electron microscopy (TEM), otherwise a powerful tool to get experimental evidence of the structural quality of the layers, interface abruptness, and estimations of the local chemical composition. In this work, we present an in-depth analysis using scanning (S)TEM of a series of Ga(Sb,Bi) epilayers and Ga(Sb,Bi)/GaSb QWs similar to those used in the recent demonstration of a mid-IR Ga(Sb,Bi)/GaSb QW laser.[3]

The samples were grown by MBE on GaSb(001) substrates. Conventional effusion cells were used for Ga and Bi, and a valved Sb-cracker cell was used for Sb supply. The substrate temperature T_s was monitored using an optical pyrometer for temperatures above 380 °C, whereas the thermocouple

[a)]Author to whom correspondence should be addressed: luna@pdi-berlin.de

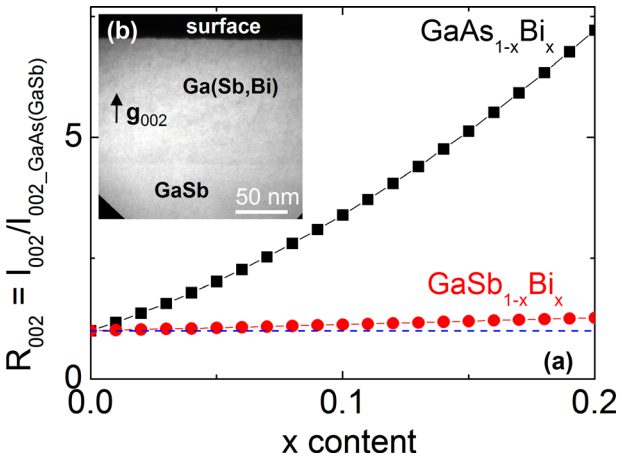

FIG. 1. (a) Estimated $\mathbf{g}_{002}$ DFTEM image contrast computed as the ratio of the diffracted intensity at the layer and at the GaSb (GaAs) reference, respectively. (b) Chemically sensitive $\mathbf{g}_{002}$ DFTEM micrograph of Ga(Sb,Bi) with 14% Bi.

temperature reading (TTR) was used as a reference for the low temperature growth of Ga(Sb,Bi). Prior to the $GaSb_{1-x}Bi_x$ growth, a ~300 nm thick GaSb buffer layer was grown at $T_s = 500\,^{\circ}C$, after which T_s was reduced to TTR = 200 °C and stabilized during 5 min. Then, the Ga, Sb, and Bi shutters were simultaneously opened for the growth of ~120 nm Ga(Sb,Bi) epilayers or 15 nm Ga(Sb,Bi)/20 nm GaSb QWs, respectively, at a growth rate of 0.3 monolayers/s (ML/s) with a V/III flux ratio close to stoichiometry. The QWs were embedded between 180 nm GaSb layers and 20 nm $AlAs_{0.08}Sb_{0.92}$ barriers grown at $T_s = 425\,^{\circ}C$ (350 °C TTR) and further capped with GaSb to avoid oxidation of the topmost Al(As,Sb) layer. The laser structure is based on such a Ga(Sb,Bi)/GaSb QW active region grown at TTR = 200 °C and sandwiched between GaSb waveguide layers and (Al,Ga)(As,Sb) cladding layers grown at the higher $T_s = 450\,^{\circ}C$. Further details on the growth conditions and samples structure are reported elsewhere.[3,12]

Cross-sectional TEM specimens were prepared in the [110] and $[\bar{1}10]$ projections by mechanical thinning, followed by Ar-ion milling. In order to minimize the sputtering damage, the Ar-ion energy was reduced to 2–0.5 keV. The samples were investigated on a JEOL 3010 microscope and on a (S)TEM JEOL 2100F microscope both operating at 200 kV. In general, chemically sensitive $\mathbf{g}_{002}$ dark-field (DF) TEM is a powerful and direct method to determine the element distribution in III–V semiconductors with zinc-blende (ZB) structure.[20,21] When 002 imaging conditions are properly set up (the specimen is tilted 8°–10° from the ⟨110⟩ zone axis towards the [100] pole, while keeping the interface edge-on),[21] the contrast directly reflects the chemical composition of the alloy. The reason is that in III–V alloys with ZB structure, the $\mathbf{g}_{002}$ diffracted intensity under kinematic approximation is proportional to the square of the structure factor, which depends on the difference in the atomic scattering factors of the alloy components. Therefore, in this "structure-factor imaging mode," the contrast mainly arises from differences in the atomic-scattering factors between the group-III and group-V elements. On the other hand, other analytical tools such as energy dispersive X-ray spectrometry (EDS) would require the use of suitable references of known compositions for a reliable determination of the chemical composition. Unfortunately, in the present situation, there is a lack of suitable references (e.g., the not-yet synthesized endpoint GaBi compound[1]), thus limiting EDS quantitative capabilities and awarding $\mathbf{g}_{002}$ DFTEM a potential suitability for chemical quantification in this material system. Furthermore, $\mathbf{g}_{002}$ DFTEM imaging is a very valuable

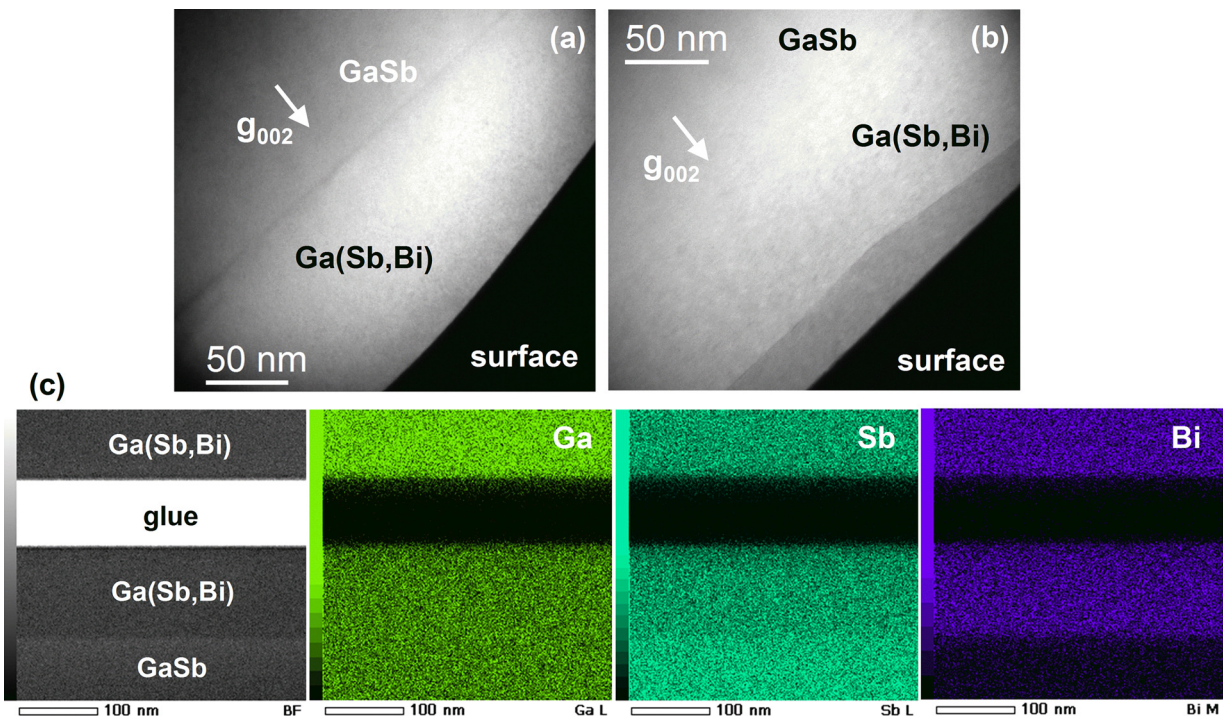

FIG. 2. (a) and (b) Chemically sensitive $\mathbf{g}_{002}$ DFTEM micrographs of the pseudomorphic Ga(Sb,Bi) epilayer with 14% Bi from an area with surface droplets, leading to thickness irregularities (a) and a "two-composition" layer (b). (c) Bright-field STEM image and EDS compositional map from a droplet-free uniform area.

technique for the investigation of compositional inhomogeneities in Ga(As,Bi)[7,8,22] since it allows the detection of small variations (around 0.5%) in the Bi content and, in particular, of composition fluctuations which cannot be detected using conventional XRD techniques.[23] Theoretical estimations of the $\mathbf{g}_{002}$ diffracted intensity in Ga(Sb,Bi) predict, however, that the intensity contrast to GaSb is extremely low, with $I_{002\text{-}GaSbBi}/I_{002\text{-}GaSb} \sim 1.19$ for Ga(Sb,Bi) with 14% Bi, which is in marked difference to Ga(As,Bi) where $I_{002\text{-}GaAsBi}/I_{002\text{-}GaAs} \sim 4.7$ for Ga(As,Bi) with 14% Bi, as observed in Fig. 1(a). This low contrast renders $\mathbf{g}_{002}$ DFTEM imaging of Ga(Sb,Bi) extremely challenging.

Figures 1(b), 2(a), and 2(b) display cross-sectional $\mathbf{g}_{002}$ DFTEM micrographs of the Ga(Sb,Bi) epilayer with 14% Bi, the maximum Bi concentration incorporated into GaSb so far. The 120 nm thick layer grows pseudomorphically on GaSb and no dislocations, or extended defects are detected. There are nevertheless droplets on the surface.[12] The areas investigated by TEM correspond to regions with a lower density of droplets. The homogeneous intensity contrast in the chemically sensitive $\mathbf{g}_{002}$ DFTEM image suggests a homogeneous layer, where no clustering or CMs are detected. Furthermore, local quantitative chemical determination from the analysis of the $\mathbf{g}_{002}$ diffracted intensity following the procedure proposed by Bithell and Stobbs[20] and using GaSb as a reference yields an average Bi content $[\mathrm{Bi}] \sim (14.2 \pm 0.8)\%$, which is in good agreement with $[\mathrm{Bi}]_{\mathrm{RBS}} = 14\%$.[12] The error bar refers to the standard deviation of the experimental data and does not include systematic errors. In the $\mathbf{g}_{002}$ DFTEM analysis, we assume that Bi incorporates substitutionally at Sb positions, as well as the validity of Vegard's law. It is worth noting here that the Bi contents determined by both RBS and XRD agree for all concentrations below ~12%. At higher compositions, however, RBS reveals a significant Bi incorporation in non-substitutional sites, causing a lattice expansion not following Vegard's law. In turn, this affects the Bi-composition deduced from XRD measurements, and for the sample considered in this paragraph, $[\mathrm{Bi}]_{\mathrm{XRD}} = 16.9\%$, while the actual value given by RBS is $[\mathrm{Bi}]_{\mathrm{RBS}} = 14\%$, as confirmed by TEM. The images in Figs. 2(a) and 2(b) evidence two interesting features: (i) there are local variations in the layer thickness ranging from 80 to 120 nm depending on the area, which seems to arise from an unintended *etching process* during growth rather than from an irregular growth rate; and (ii) the presence of a "two-composition layer" with a second layer of unknown composition close to the sample surface. The darker contrast of this second layer would suggest that it is Bi-depleted. This strong reduction in the Bi content should be detectable by EDS and high-angle annular dark-field (HAADF) which, however, are not sufficiently informative to identify any change in the composition. On the other hand, the systematic dark and well-delimited contrast in this region, even darker than for GaSb, also points to the possibility of a layer with a different point defect density than the underlying Ga(Sb,Bi). In the analysis of $\mathbf{g}_{002}$ DFTEM micrographs, we assume Bi substitutional incorporation at the Sb position and any deviation from it (e.g., due to antisites, interstitial Bi) would definitively affect the contrast. Note that $\mathbf{g}_{002}$ DFTEM "structure-factor imaging" is highly sensitive to the presence of interstitials in the dilute magnetic semiconductor (Ga,Mn)As.[24] Incidentally, RBS measurements of the sample seem to indicate a higher interstitial rate than in layers with a smaller Bi content (11%–12% Bi) which, interestingly, do not show this "two-composition" layer or the "etching features" as shown in the overview images in Fig. 3. The presence of a "two-composition layer" (or sequences of layers with different Bi contents and a morphology similar to the one detected here) has been already observed in dilute bismide epilayers,[9,17,25,26] in most cases in connection with the existence of Bi droplets on the surface.[17,25–27] The role of surface droplets during growth of dilute bismides and its impact on Bi incorporation inhomogeneities are currently under active investigation.[9,17,18,25–27] Hence, a comprehensive and dedicated study of the effect of surface droplets on the observed morphology depicted in Figs. 2(a), 2(b), and 3(a) is definitively necessary and will be considered in future investigations. At present, we can only speculate that both features (i) and (ii) seem to correlate with the (almost unavoidable) presence of surface droplets for this very high Bi content sample since none of these features could be detected in the (surface) droplet-free Ga(Sb,Bi) epilayers with 11%–12% Bi [cf. Fig. 3(b)].

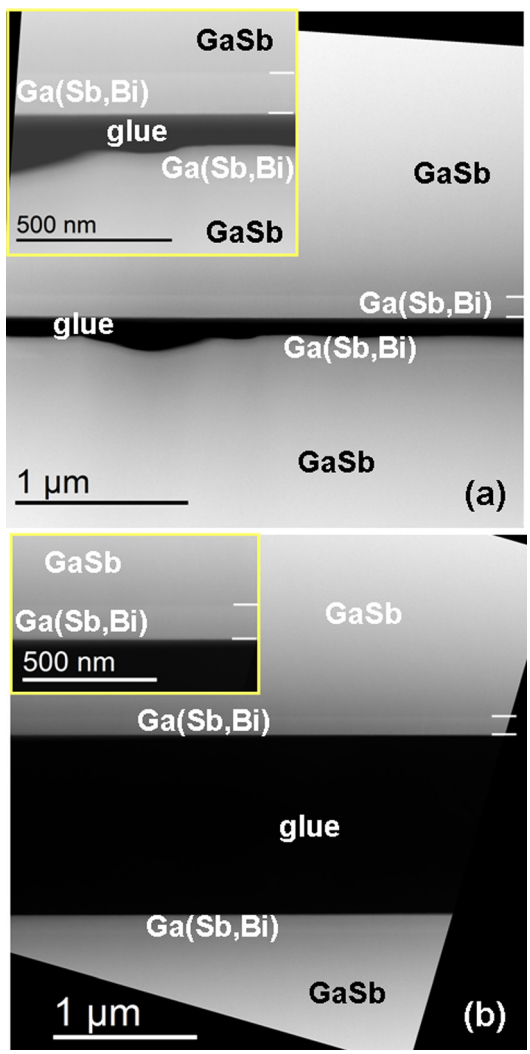

FIG. 3. HAADF overview images of Ga(Sb,Bi) epilayers with about 14% Bi (a) and 11%–12% Bi (b). The HAADF micrographs in the insets are taken at a higher magnification.

On the other hand, the low contrast in $\mathbf{g}_{002}$ DFTEM imaging of Ga(Sb,Bi) renders the detection of CMs an arduous task. It has been reported that the amplitude of lateral CMs in Ga(As,Bi) is about $\Delta[\mathrm{Bi}]/[\mathrm{Bi}] \sim 30\%$.[7,8,23] In Ga(As,Bi) with an average Bi content of $[\mathrm{Bi}]_{\mathrm{avg}} = 5\%$, the presence of a 30% modulation induces a contrast of about 16%, which is readily detectable (we estimate that 3–3.6% contrast is the lower limit of detection that we achieve using $\mathbf{g}_{002}$ DFTEM[28]). Assuming that the amplitude of CMs in Ga(Sb,Bi) is as large as that in Ga(As,Bi), a 30% modulation in Ga(Sb,Bi) with $[\mathrm{Bi}]_{\mathrm{avg}} = 14\%$ (or in Ga(Sb,Bi) with $[\mathrm{Bi}]_{\mathrm{avg}} = 11.5\%$ Bi, as a representative composition for the QW samples) would induce a contrast of about 5.7% (5.1%), which is significantly smaller than in Ga(As,Bi) but still detectable. Yet, a 20% modulation in Ga(Sb,Bi) with 11.5% or 14% Bi would be at our limit of detection, with 3.4% contrast. CMs below 20% would, however, be very challenging to detect since they do not produce enough contrast. EDS measurements performed in homogeneous areas as those identified in the overview image in Fig. 3(a) [cf. Fig. 1(b) for $\mathbf{g}_{002}$ DFTEM of such an area] without surface irregularities or a "two-composition layer" are shown in Fig. 2(c). The EDS maps also evidence a homogeneous layer, at least at this level of detection, where the Ga(Sb,Bi) layer is well-delimitated from the adjacent GaSb, as indicated by the decrease in the $L_{\alpha 1}$ peak Sb signal and the concomitant increase in the intensity of the Bi $M_{\alpha 1}$ peak. HAADF micrographs [cf. Fig. 3(a) at the areas of regular layer thickness] with so-called Z-contrast provide similar information to $\mathbf{g}_{002}$ DFTEM and EDS: a homogeneous layer, where no clusters and CMs are detected. Hence, from the combined information provided by $\mathbf{g}_{002}$ DFTEM, EDS, and HAADF, we conclude that, except in areas with surface irregularities and a "two-composition layer," we deal with homogeneous Ga(Sb,Bi) epilayers where CMs are below 20%.

The high structural quality of the material is also reflected in the Ga(Sb,Bi)/GaSb QWs comprising a reference structure and the laser active zone. Again, no extended defects, clustering, or CMs are detected. In addition, the QWs exhibit regular and homogeneous morphologies including smooth interfaces. Figures 4(a) and 4(b) display bright-field and $\mathbf{g}_{002}$ DFTEM micrographs of the QWs in the reference sample. The thickness of the QWs (in the growth sequence) ranges from (14.5 ± 0.4) nm, (14.6 ± 0.4) nm, and (14.8 ± 0.4) nm, respectively. The three QWs are affected by slight thickness fluctuations (on the 100 nm length scale of the TEM image), as evidenced in Fig. 4. Quantitative determination of the Bi content from the analysis of $\mathbf{g}_{002}$ DFTEM micrographs yields $[\mathrm{Bi}]_{\mathrm{TEM}} = (11.8 \pm 1.4)\%$, which is in agreement with the average composition deduced from XRD.[3] Figure 4(d) shows a representative local Bi distribution profile across the QW obtained from the analysis of the $\mathbf{g}_{002}$ diffracted intensity.[8,20] It turns out that, in analogy with other III–V semiconductor systems, the Ga(Sb,Bi)/GaSb interfaces are strikingly well defined by a sigmoidal function.[29] This is shown in Fig. 4(d) which displays the experimental profile and the fitting to the sigmoidal function describing the intrinsic broadening at semiconductor heterointerfaces.[29] The perfect fit to a sigmoidal function further allows quantification of the chemical interface width, which in this case ranges between 2.2 and 2.7 nm (defined by 10%–90% criterion). Note that the estimated width is on the same order as the chemical interface in other III–V heterointerfaces, e.g., 2.1 nm for high quality (Al,Ga)As/GaAs.[29] We note that although the QWs are homogeneous in composition, the presence of lateral thickness fluctuations and, in particular, the non-steady interface width may impact the

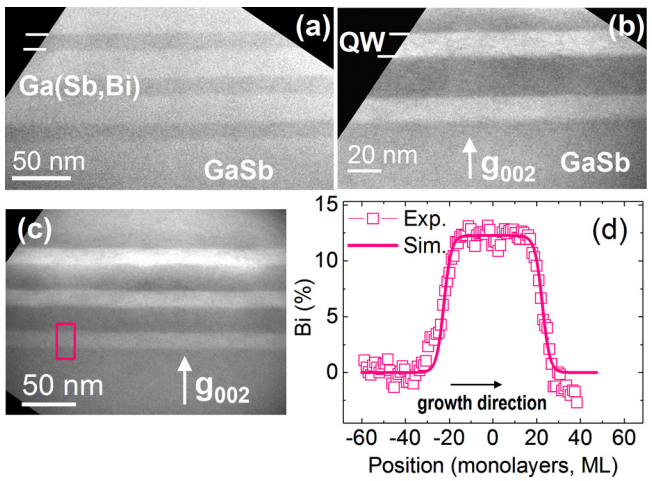

FIG. 4. (a) Bright-field and (b) and (c) chemically sensitive $\mathbf{g}_{002}$ DFTEM micrographs of the Ga(Sb,Bi)/GaSb QWs in a reference sample, together with (d) the Bi composition profile extracted from the analysis of the $\mathbf{g}_{002}$ DFTEM diffracted intensity in the area marked in (c). The experimental data are fitted to a sigmoidal function.

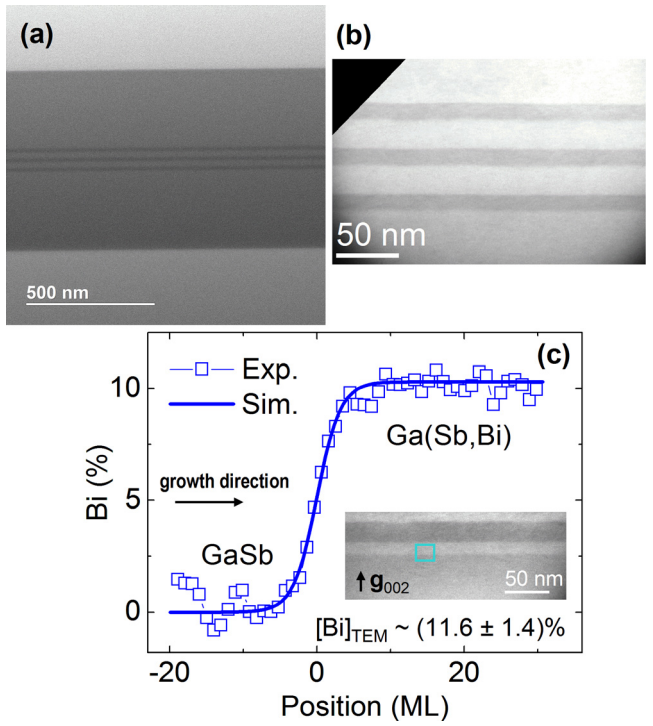

FIG. 5. (a) Bright-field STEM overview of the laser structure with (b) an enlarged bright-field micrograph of the QWs comprising the active zone. (c) Bi distribution profile at the Ga(Sb,Bi)-on-GaSb interface at QWs in the laser structure, extracted from the analysis of the $\mathbf{g}_{002}$ DFTEM diffracted intensity. The experimental data are fitted to a sigmoidal function. The abrupt interfaces at the laser structure are similar to those in the reference samples and demonstrate that the *in-situ* annealing during MBE growth of the top cladding and contact layers seems not to have a detrimental effect, at least in terms of interface quality.

optical properties.[3,4,12] This valuable information discloses the critical features to further improve the homogeneity of the QWs in terms of thickness and interface width. Both Ga(Sb,Bi)-on-GaSb and GaSb-on-Ga(Sb,Bi) interfaces are rather symmetric and exhibit a similar interface width, which also rules out the presence of strong Bi segregation.[8,22]

In general, there are no visible differences in the morphology of the QWs in the reference sample and in the laser structure (cf. Figs. 4 and 5), which demonstrates that in spite of the growth challenges, the degree of reproducibility is remarkable. Quantitative determination of the Bi content from the analysis of chemically sensitive $\mathbf{g}_{002}$ DFTEM micrographs yields $[\mathrm{Bi}] = (11.6 \pm 1.4)\%$. Slight fluctuations in QW thickness and interface width are also perceived in the laser structure. In this case, the interface width ranges between 2 and 2.8 nm, in the 10–90% criterion, without any signature of Bi surface segregation. Finally, the abrupt interfaces in the laser structure also demonstrate that *in-situ* annealing during MBE growth of the top cladding and contact layers at the higher $T_s = 450\,^{\circ}\mathrm{C}$ does not have a detrimental effect on the layers, at least in terms of interface quality. Nevertheless, reducing thickness and interfacial fluctuations would probably improve laser performances.

In summary, first investigations of the microstructure and chemical homogeneity of the emerging dilute bismide compound Ga(Sb,Bi) demonstrate its high quality, high stability, and feasibility for use in the active zone of optoelectronic devices operating in the mid-IR. From the combined information of several chemically sensitive (S)TEM techniques, we conclude that in areas without surface irregularities, Ga(Sb,Bi) layers are homogeneous with CMs below 20%. In addition, the abrupt interfaces at Ga(Sb,Bi)/GaSb QWs are stable against the higher growth temperature of the top layers, e.g., in a laser structure. Although it is obvious that further refinements are required (e.g., in order to improve the homogeneity of the interfaces), our results demonstrate that Ga(Sb,Bi) is a promising material for optoelectronic applications.

The authors thank Astrid Pfeiffer for technical assistance with TEM and, in particular, Sabine Krauß for her dedicated TEM specimen preparation. The authors thank Guanhui Gao for a critical reading of this manuscript. Part of this work was supported by the French program on "Investments for the future" (Equipex EXTRA, ANR-11-EQPX-0016) and by the French ANR (Project BIOMAN, No. ANR-15-CE24-0001).

[1]L. Wang, L. Zhang, L. Yue, D. Liang, X. Chen, Y. Li, P. Lu, J. Shao, and S. Wang, Crystals **7**, 63 (2017).
[2]T. Tiedje, E. C. Young, and A. Mascarenhas, Int. J. Nanotechnol. **5**, 963 (2008).
[3]O. Delorme, L. Cerutti, E. Luna, G. Narcy, A. Trampert, E. Tournié, and J.-B. Rodriguez, Appl. Phys. Lett. **110**, 222106 (2017).
[4]A. Trampert, J.-M. Chauveau, K. H. Ploog, E. Tournié, and A. Guzmán, J. Vac. Sci. Technol. B **22**, 2195 (2004).
[5]A. G. Norman, R. France, and A. J. Ptak, J. Vac. Sci. Technol. B **29**, 03C121 (2011).
[6]D. F. Reyes, F. Bastiman, C. J. Hunter, D. L. Sales, A. M. Sánchez, J. P. R. David, and D. González, Nanoscale Res. Lett. **9**, 23 (2014).
[7]E. Luna, M. Wu, J. Puustinen, M. Guina, and A. Trampert, J. Appl. Phys. **117**, 185302 (2015).
[8]E. Luna, M. Wu, M. Hanke, J. Puustinen, M. Guina, and A. Trampert, Nanotechnology **27**, 325603 (2016).
[9]C. R. Tait, L. Yan, and J. M. Millunchick, Appl. Phys. Lett. **111**, 042105 (2017).
[10]S. K. Das, T. D. Das, S. Dhar, M. de la Mare, and A. Krier, Infrared Phys. Technol. **55**, 156 (2012).
[11]Y. Song, S. Wang, I. S. Roy, P. Shi, and A. Hallen, J. Vac. Sci. Technol. B **30**, 02B114 (2012).
[12]O. Delorme, L. Cerutti, E. Tournié, and J.-B. Rodriguez, J. Cryst. Growth **477**, 144 (2017).
[13]R. B. Lewis, M. Masnadi-Shirazi, and T. Tiedje, Appl. Phys. Lett. **101**, 082112 (2012).
[14]M. K. Rajpalke, W. M. Linhart, M. Birkett, K. M. Yu, D. O. Scanlon, J. Buckeridge, T. S. Jones, M. J. Ashwin, and T. D. Veal, Appl. Phys. Lett. **103**, 142106 (2013).
[15]M. K. Rajpalke, W. M. Linhart, M. Birkett, K. M. Yu, J. Alaria, J. Kopaczek, R. Kudrawiec, T. S. Jones, M. J. Ashwin, and T. D. Veal, J. Appl. Phys. **116**, 043511 (2014).
[16]M. K. Rajpalke, W. M. Linhart, K. M. Yu, T. S. Jones, M. J. Ashwin, and T. D. Veal, J. Cryst. Growth **425**, 241 (2015).
[17]L. Yue, X. Chen, Y. Zhang, F. Zhang, L. Wang, J. Shao, and S. Wang, J. Alloys Compd. **742**, 780 (2018).
[18]A. Duzik and J. M. Millunchick, J. Cryst. Growth **390**, 5 (2014).
[19]Y. Zhang, L. Yue, X. Chen, J. Shao, X. Ou, and S. Wang, J. Alloys Compd. **744**, 667 (2018).
[20]E. G. Bithell and W. M. Stobbs, Philos. Mag. A **60**, 39 (1989).
[21]J. Lu, E. Luna, T. Aoki, E. H. Steenbergen, Y.-H. Zhang, and D. J. Smith, J. Appl. Phys. **119**, 095702 (2016).
[22]P. K. Patil, E. Luna, T. Matsuda, K. Yamada, K. Kamiya, F. Ishikawa, and S. Shimomura, Nanotechnology **28**, 105702 (2017).
[23]M. Wu, M. Hanke, E. Luna, J. Puustinen, M. Guina, and A. Trampert, Nanotechnology **26**, 425701 (2015).
[24]F. Glas, G. Patriarche, L. Largeau, and A. Lemaître, Phys. Rev. Lett. **93**, 086107 (2004).
[25]J. A. Steele, R. A. Lewis, J. Horvat, M. J. B. Nancarrow, M. Henini, D. Fan, Y. I. Mazur, M. Schmidbauer, M. E. Ware, S.-Q. Yu, and G. J. Salamo, Sci. Rep. **6**, 28860 (2016).
[26]A. W. Wood, K. Collar, J. Li, A. S. Brown, and S. E. Babcock, Nanotechnology **27**, 115704 (2016).
[27]C. R. Tait and J. M. Millunchick, J. Appl. Phys. **119**, 215302 (2016).
[28]E. Luna, R. Gargallo-Caballero, F. Ishikawa, and A. Trampert, Appl. Phys. Lett. **110**, 201906 (2017).
[29]E. Luna, A. Guzmán, A. Trampert, and G. Álvarez, Phys. Rev. Lett. **109**, 126101 (2012).